



HAL
open science

Structuring wheat dough using a thermomechanical process, from liquid food to 3D-printable food material

Laurena Masbernat, Sophie Berland, Cassandre Leverrier, Gabrielle Moulin,
Camille Michon, Giana Almeida

► To cite this version:

Laurena Masbernat, Sophie Berland, Cassandre Leverrier, Gabrielle Moulin, Camille Michon, et al.. Structuring wheat dough using a thermomechanical process, from liquid food to 3D-printable food material. *Journal of Food Engineering*, 2021, 310, pp.110696. 10.1016/j.jfoodeng.2021.110696 . hal-03965620

HAL Id: hal-03965620

<https://hal.science/hal-03965620v1>

Submitted on 13 Jun 2023

HAL is a multi-disciplinary open access archive for the deposit and dissemination of scientific research documents, whether they are published or not. The documents may come from teaching and research institutions in France or abroad, or from public or private research centers.

L'archive ouverte pluridisciplinaire **HAL**, est destinée au dépôt et à la diffusion de documents scientifiques de niveau recherche, publiés ou non, émanant des établissements d'enseignement et de recherche français ou étrangers, des laboratoires publics ou privés.



Distributed under a Creative Commons Attribution - NonCommercial 4.0 International License

1 **Structuring wheat dough using a thermomechanical process, from liquid food to 3D-printable food**
2 **material**

3 Laurena Masbernat ^a, Sophie Berland ^a, Cassandre Leverrier ^a, Gabrielle Moulin ^a, Camille

4 Michon ^a, Giana Almeida ^a

5 ^a Université Paris-Saclay, INRAE, AgroParisTech, UMR SayFood, 91300, Massy, France.

6 Corresponding authors: giana.perre@agroparistech.fr

7 *Abstract*

8 **In extrusion printing**, the printability of food materials depends on the rheology of the food under
9 shearing when extruded, and at rest, post-deposition. Piloting food microstructure to provide
10 rheological properties compatible with 3D extrusion printing is a major challenge. Microstructure,
11 rheology, and printability of wheat-flour based materials with varying concentrations of flour, sugar,
12 oil, and water were studied. Materials were obtained by heating and shearing doughs with a
13 moisture content above 55% (wb). The processed doughs were structured as closely-packed particles
14 made of swollen gelatinized starch granules glued **in a denatured proteins network**. These materials
15 were easily extruded in **self-supporting layers** by a 3D food-printer and formed stable objects with
16 precise dimensions. The water/flour ratio played a crucial role in the structure of the wheat
17 materials, impacting the storage modulus (G'), $\tan \delta$ and printability. This work highlights the
18 importance of $\tan \delta$ in predicting the ability of food materials to hold its 3D structure.

19 **Keywords:** 3D printing, microscopy, rheology, starch, thermomechanical process, water

20 *Highlights*

- 21 • Thermomechanical processing of doughs produced wheat-based printable materials
- 22 • Dough particles were made of swollen starch glued by denatured proteins
- 23 • Excess water, oil and sugar had no effect on rheology or printability
- 24 • The water/flour ratio is an important parameter to pilot a material's printability
- 25 • **Tan δ is a relevant indicator to predict the post-deposition behavior of materials**

26

27 I. Introduction

28 The growing interest of researchers and industry in 3D food printing in the last five years led to
29 advances in the technology and to the formulation of a variety of printable edible materials.
30 Extrusion printing, which consists in forcing material through a die opening, was first used to print
31 thermoplastics (Turner et al., 2014). Then, edible 3D objects made of food materials with a pasty
32 texture were printed including wheat dough (Severini et al., 2016; Yang et al., 2018), mashed
33 potatoes (Liu et al., 2017) and surimi paste (Wang et al., 2018). Studies of 3D printing of polylactic
34 acid (PLA), a widely used thermoplastic in design and prototyping, revealed a correlation between
35 the viscosity of a material and its ability to be printed (Bakrani et al., 2019). At room temperature,
36 PLA is a solid-like material and can only be extruded when heated above its melting transition
37 temperature (about 200 °C for semi-crystalline PLA) when its viscosity is lowered to about 2,000 Pa.s
38 (Bakrani et al., 2019). When deposited on the printing plate after extrusion, the material rapidly
39 solidifies by going through the glass transition while cooling. To form an object in volume, the
40 viscosity of the material must be high enough to form a self-supporting layer, i.e., not deform under
41 its own weight or the weight of subsequently deposited layers, until the transition to a solid state is
42 achieved (Godoi et al., 2016). On the other hand, printing a high viscosity material requires
43 considerable energy and can increase pressure inside the printer which then affects the printing flow
44 rate. Printability defines the ability of the material to be extruded by the printer and to maintain its
45 printed structure post-deposition (Godoi et al., 2016). Thus, shear-thinning fluids showing high
46 viscosity at very low shear rates, but whose viscosity is several orders of magnitude lower during
47 extrusion, could be compatible with 3D printing. Wheat flour dough was one of the first food
48 material successfully 3D printed. To some extent, the doughs of cereal products combine the shear-
49 thinning behavior required during the extrusion step of the printing process (Jiang et al., 2019). These
50 properties are related to the organization of the wheat flour components in the dough combined
51 with the structuring effect of proteins at room temperature obtained by kneading and, to a lesser

52 extent, of the numerous starch granules dispersed within the dough. The organization of the gluten
53 proteins depends mostly on the water content and the mixing process, and can lead to the formation
54 of an elastic network of proteins in which starch granules are embedded (depending on the quality of
55 the protein and the type of wheat) (Auger et al., 2008). So far, wheat flour has been added in the
56 recipes of printable materials because of the ability of the compounds in the flour to bind water, and
57 the ability of the proteins in the flour to interact and form a viscoelastic gluten network (Kim et al.,
58 2019; Severini et al., 2018, 2016; Yang et al., 2018; Zhang et al., 2018). However, to our knowledge,
59 no works have explored changes in the properties of the dough under heat treatment at water
60 contents higher than 55 wt% for which no gluten network can be formed, whereas, the swelling of
61 starch in such wheat doughs may provide an interesting path for the development of printable food
62 materials.

63 Wheat starch is a well-known food texturing agent (Rapaille and Vanhemelrijck, 1997) and a major
64 component of wheat flour (between 70 to 80% of dry mass). Wheat starch is composed of glucose
65 polymers, amylose, and amylopectin, organized in a semi-crystalline structure in the native starch
66 granule. Under heat treatment and in presence of water, the starch absorbs the water from the
67 medium, loses its semi-crystalline structure and swells. This phenomenon, which affects the
68 structure of the granule, is referred to as starch gelatinization. Depending on the concentration of
69 starch and on the heating parameters, the swollen starch granules may come into contact with one
70 another. They then form a closely-packed system of granules that occupies a much larger volume
71 than the one occupied by the continuous phase made of denatured gluten proteins that covers the
72 starch granules (Bagley and Christianson, 1982; Hermansson and Svegmarm, 1996).

73 The effect of the composition of the dough after the addition of texturizers, sugars and fat on the
74 printability of wheat doughs has been studied by several authors (Kim et al., 2019; Yang et al., 2018).
75 The addition of sucrose and fat are known to reduce the viscosity and elasticity of the dough at room
76 temperature (Hesso et al., 2015; Maache-Rezzoug et al., 1998). Depending on the composition of the

77 dough, upon heating, the addition of sugar and oil affects starch gelatinization kinetics (Abboud and
78 Hosenev, 1984; Perry and Donald, 2002) and delays the swelling of the granules until higher
79 temperatures are reached (Bean and Yamazaki, 1978). In the same process, the volume fraction of
80 the starch granules may differ depending on the concentration of sucrose or oil, and consequently
81 alter the properties of the heated dough.

82 If the system is sheared during heating, ongoing starch pasting and denaturation of the gluten
83 network lead to the formation of a gel that is cut into numerous sticky particles. The rheology of
84 closely-packed particulate systems is driven by the volume fraction, *i.e.*, the volume occupied by the
85 particles, the spatial organization, the contact interactions, and the shape and the rigidity of the
86 particles (Coussot and Ancey, 1999; Quemada, 1977). Rheology is most often characterized by a yield
87 stress and shear-thinning behavior beyond this stress. At low shear rates, the rheology of a closely
88 packed particle system is dominated by contact interactions, in other words, friction between the
89 particles (Coussot and Ancey, 1999) and the spatial arrangement of the particles, which might be
90 randomly close-packed or follow a pattern (Quemada, 2006). Under shearing, the stabilized
91 particulate network has to be broken by the action of stress applied above the system yield stress to
92 allow the system to flow with increasing hydrodynamic interactions, *i.e.*, the energy dissipated by
93 viscous frictions between the medium and particles (Quemada, 1977). The state of the surface and
94 the rigidity of the particles are important parameters in the rheology of concentrated suspensions, as
95 they define contact interactions and the ability of the particles to deform and align with the flow with
96 major effects on the shear-thinning behavior of the system.

97 The dough obtained after heating under shear can be compared with a system of closely-packed
98 particles that stick together due to the denatured proteins that coat them. These particles are also
99 rather soft due to the properties of the swollen starch granules and to the denatured protein
100 network in which they are stuck. To date, this system has not been well characterized in the
101 literature. Indeed, particles involved in concentrated food suspensions, such as starch paste or

102 vegetable purees, may be deformable, but were previously not defined as being sticky (Leverrier et
103 al., 2016; Rao, 2007). In another field of application, the stickiness of clay particles was made visible
104 by slow dispersion of the particles under shearing, but clay particles are much more rigid than dough
105 particles (Mongondry et al., 2005).

106 The aim of the present study was to develop a wheat-based material compatible with 3D printing
107 extrusion, using the structuring properties of starch and proteins while heating under shearing. A lab-
108 scale thermomechanical process was developed that enabled heat induced changes in the
109 organization of starch and proteins to increase wheat dough viscosity. The roles of starch, protein,
110 water and additional sucrose and oil in structuring were analyzed. The rheological properties of the
111 resulting material were investigated and compared to its printability.

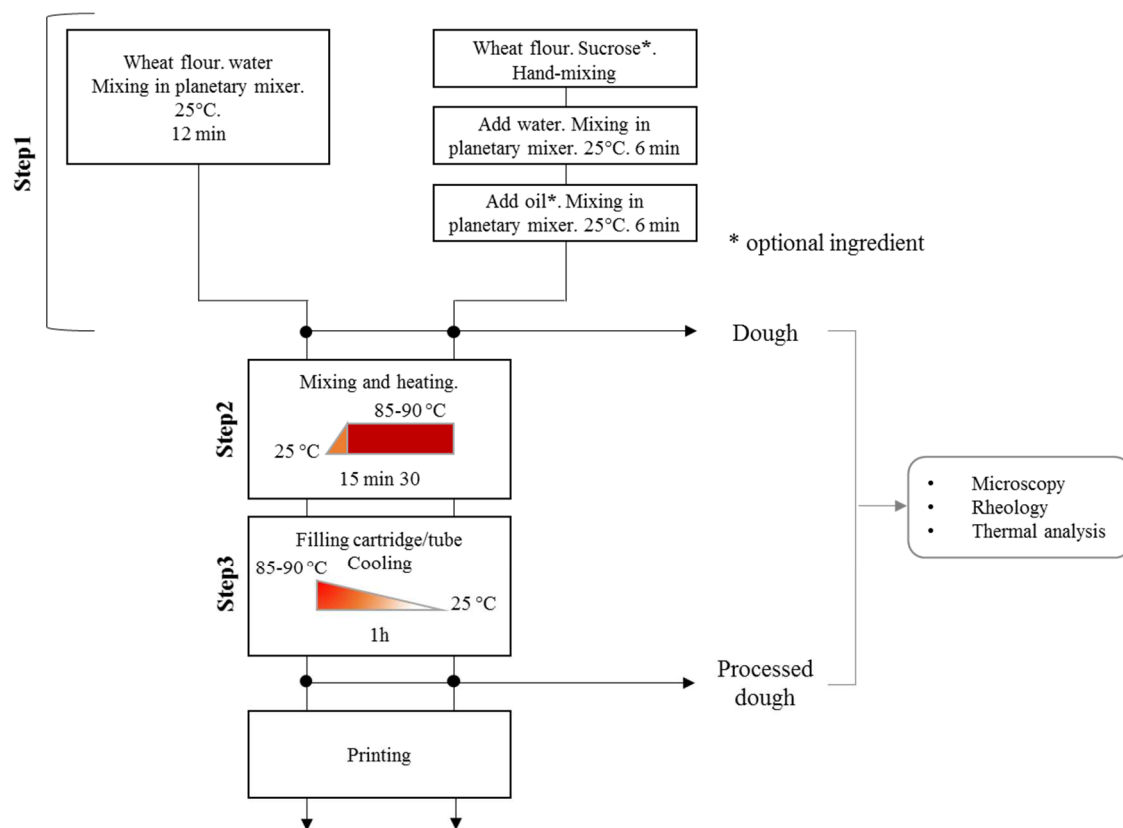
112

113 **II. Materials and methods**

114 *II.1. Materials and preparation of printable food materials*

115 Wheat-based printable materials were prepared by mixing **all-purpose wheat flour (soft wheat)**, (Les
116 fournils du Val de Loire, France) with deionized water, with the addition of commercial sugar
117 (sucrose) (Saint-Louis) and sunflower oil (Cora). The water content of the wheat flour was 14.55
118 ± 0.01 g per 100 g flour (ISO 712:2009). Total protein content was 11.29 ± 0.04 g per 100 g dry flour
119 (ISO 16634-2) (Qualtech, France) and **ash content was 0.58 ± 0.01 g per 100 g dry flour (ISO 18122)**.

120 Powdered sugar and sunflower oil were stored in a dry place at room temperature and wheat flour
121 was stored in airtight plastic buckets at -30 °C. All the ingredients were allowed to return to room
122 temperature before use. The materials to be printed were obtained in the 3-step process described
123 in Figure 1.



124

125 *Figure 1: Experimental design to produce wheat flour-based printable material and characterization methods*

126

127 The first step was mixing the ingredients for 12 min in a 5K45SS EOB CLASSIC planetary mixer fitted
 128 with a paddle (KitchenAid, USA) at room temperature at speed 4 (about 120 rpm). The second step
 129 was a thermomechanical process performed in a Thermomix (TM5, Vorwek, Germany) fitted with an
 130 anchor device for 15.5 min at **speed 1 (100 rpm)** while the temperature was increased from 25 °C to
 131 the set-point temperature of 85 °C or 90 °C. **These process parameters were chosen after preliminary**
 132 **experiments and were set to allow heat-induced modifications of starch and proteins, without**
 133 **significant evaporation of water and hence drying of the dough.** In the bowl, the heat was transferred
 134 in the dough from the bottom to the top. The third and last step consisted in filling the printing
 135 cartridge or tube using a pastry bag and leaving it to cool for 1 h at room temperature so the
 136 temperature of the processed dough reached about 25 °C before further measurements and
 137 printing.

138 A dough with 65 wt% water was chosen as reference. This water content allowed us to obtain a post
 139 heating viscosity that was compatible with lab-scale production. Changes in temperature and in the
 140 rheological properties during step 2 were studied by stopping the process at different times. The
 141 temperature of the dough was measured immediately after the process was stopped. The rheology
 142 was characterized after cooling the sample to room temperature.

143 In order to investigate the effect of ingredients on the 3D printing properties of the processed dough,
 144 three levels of sunflower oil, three levels of sucrose and six levels of water were tested. Water,
 145 sucrose, and oil concentrations were varied in the ranges 55-80.7 wt%, 0-18 wt% and 0-15 wt%,
 146 respectively (Table 1). The highest concentrations of oil (15%) and sucrose (18%) in the recipes we
 147 tested are the oil and sucrose contents found in existing products, such as laminated biscuits (Charun
 148 and Morel, 2001). All the compositions of the formulations are summarized in Table 1.

149 *Table 1: Formulations used in this study. The formulations are ordered according the ratio of water to flour. The ingredients*
 150 *are expressed as a percent, in g of ingredient/100 g of total formulation. The water/flour ratio is the ratio of the weight of*
 151 *added water to the weight of wheat flour.*

Code number	Water/Flour (w/w)	Water content (%)	Added water (%)	Sucrose (%)	Oil (%)
0	1.12	60	52,8	0	0
1	1.35	60	54.0	6	0
2	1.43	65	58.8	0	0
3	1.67	60	55.0	12	0
4	1.68	55	50.5	12	7.5
5	1.76	65	59.9	6	0
6	1.83	70	64.7	0	0
7	1.86	65	60.2	0	7.5
8	2.25	65	60.9	12	0
9	2.34	74.6	70.1	0	0
10	2.34	60	56.4	12	7.5
11	2.55	70	67.5	6	0
12	2.61	65	61.5	0	15
13	3.10	65	62.0	18	0
14	3.41	80.7	77.3	0	0
15	3.41	65	62.2	12	7.5

152

153

154

155 *II.2. Printing process and evaluation of printing quality*

156 The warm processed dough was used to fill the cartridge (60 mL syringe, BD Plastipak, USA) that was
157 plugged into a prototype 3D food printer designed by Dagoma (Roubaix, France). The printing
158 process consists in the extrusion of the material stored in the cartridge by a piston. The syringe is
159 held vertically on the printer axis parallel to the printer plate (X axis). It moves laterally and vertically
160 (Z axis) while the printing bed moves on the Y axis orthogonal to the X axis. The piston is in contact
161 with the surface of the material with the larger diameter of the syringe and moves toward the
162 smaller diameter (or bottom of the syringe). The end diameter of the syringe is 3.7 mm, which
163 defines the width of the smallest layer that can be printed using these parameters. The models to be
164 printed were drawn on Tinkercad (online open access software, Autodesk, USA). The models were
165 loaded in Cura software interface (version 2.6.2, Ultimaker, NL) in which the printer and material
166 profiles were downloaded. The script for the nozzle and printer plate movements were created by
167 the software under gcode format. The height of the deposited layer was 2 mm and of the width 3.7
168 mm. The height of the layer was reduced to increase adhesion between layers and the printing
169 resolution. Depending on the object, the infill percentage varied from 100% (object is full) to 0%
170 (only the external walls are printed). All printings were carried out at 25 °C at a printing speed of 5
171 mm/s (for walls and infill layers). Pictures of the printed objects were taken after printing. The
172 dimensions of the object were measured using a caliper (Mitutoyo, Absolute Digimatic) immediately
173 after printing and again five minutes later. **The printing was assumed to be of good quality when (1)**
174 **the extruded layer formed a continuous smooth line, (2) the dimensions of the object were similar to**
175 **the dimensions of the digital model (with a tolerance of less than $\pm 20\%$ of deviation, given the**
176 **complexity of the printed structures) (Yang et al., 2018) and (3) the dimensions of the structure**
177 **remained unchanged after 5 min of observation.**

178 *II.3. Thermal analysis (differential scanning calorimetry)*

179 A power-compensated DSC calorimeter equipped with an autosampler (Q100 DSC, TA instruments,
180 Newcastle, UK) was used. Temperature and enthalpy parameters were calculated using the melting
181 transition of indium ($T_0= 156.6^\circ\text{C}$; $\Delta H= 28.5 \text{ J/g}$). An empty sample pan was used as reference and
182 nitrogen was used as the purge gas to cool the system down. Between 3 and 10 mg of product
183 (dough or processed dough, Figure 1) were weighed in aluminum pans. The samples completely
184 covered the bottom of the pans. A few drops of water were added to the pans containing samples of
185 processed doughs to allow further gelatinization in the processed doughs (final weight < 12 mg). The
186 pans were then heat-sealed and left to rest at 4°C for 10 h to let the water diffuse into the processed
187 dough. The DSC protocol began by cooling the samples to 0°C before heating them to 150°C at
188 $10^\circ\text{C}/\text{min}$. Thermograms were used to determine the temperature transition and enthalpy (ΔH) of
189 starch gelatinization. T_{onset} is the temperature required to trigger gelatinization and T_{Max} is the
190 temperature at which gelatinization is maximum. The enthalpies are converted from J/g of product
191 to J/g of starch, considering that starch represents 70% on a wet basis of the wheat flour used. The
192 degree of starch gelatinization in processed dough, G, is determined by the ratio of enthalpies
193 measured in doughs and processed dough, ΔH_D and ΔH_{pD} , respectively (Eq.1)

$$194 \quad G = 100 * (\Delta H_D - \Delta H_{pD}) / (\Delta H_D) \quad (1)$$

195 **By convention, the starch was considered to be completely gelatinized when the indicator G was**
196 **equal to 100% with a margin of 5%, i.e., for all the values of G greater than or equal to 95%. For G <**
197 **95%, starch was defined as partially or not gelatinized, no distinction being made between the two.**

198 *II.4. Microscopy*

199 Wheat starch granules were observed with an optical microscope (Olympus, Japan) at X50
200 magnification under polarized and non-polarized lights. **Samples of dough and processed dough**
201 **weighing approx.. 0.1 g were collected at different locations in the bowl and deposited on a slide.**

202 Using a 5-mL plastic Pasteur pipette, two drops of distilled water of about 0.1 mL were placed on top
203 of the samples to dilute the samples before the slide was covered with a cover slip.

204 The organization of the proteins in the material at 65 wt% of water was observed with a confocal
205 laser scattering microscope (CLSM) (Leica TC SP8 Leica, Germany). Using 250 μm thick spacers, the
206 material was put on the lamella and 2 μL of Dylight 488 was poured on top of the dough to label the
207 proteins. The stain was excited using a laser with a wavelength of 488 nm and the emitted
208 fluorescence was detected in the range of 496 to 576 nm. Pictures were taken at X10 magnification.

209 *II.5. Rheological analysis*

210 Back extrusion

211 The rheology of the processed doughs at large deformations was investigated using the back
212 extrusion method in a texture analyzer (TaHD, Stable Micro System, UK). About 35g of material were
213 poured into 40-mL plastic tubes and compressed by a piston (annulus gap of 1.5 mm) at a crosshead
214 speed of 1 mm/s applied along the 35 mm of depth. The tubes were filled with the hot processed
215 dough obtained in step 2 and cooled in the tube to room temperature. Because of the method
216 artifact, the volume filling of the tubes was kept constant in all experiments. **During compression, the**
217 **normal force (N) increased quite linearly until it reached a plateau.** The normal resistance force to
218 the flow in the annulus gap (F_M) was defined as the mean value calculated between 10 and 20 mm of
219 penetration in the sample, values for which the flowing stage (**corresponding to the plateau**) was
220 obtained in all samples (Moussier et al., 2019). Measurements were made in triplicate on at least two
221 different products.

222 Temperature and frequency sweep tests

223 Rheological measurements under dynamic oscillations were made using a dynamic stress rheometer
224 Carri-Med CLS² 100 (TA Instruments, USA) fitted with a cone-plate geometry (diameter: 4 cm, angle:
225 4° and truncation: 106 μm). Dough samples were heated from 25 to 85 °C during temperature sweep
226 tests performed at 1Hz, 5 °C/min and 0.2% of maximum strain amplitude. These conditions were

227 chosen in the linear domain (identified by preliminary strain sweeps, data not shown). Frequency
228 sweep tests conducted in the range 0.1 to 10 Hz, at 20 °C and 0.2% of strain showed that all the
229 processed dough spectra were the same shape, with higher elastic modulus (G') than loss modulus
230 (G'') over the frequency range. Thus, results at 1 Hz allowed comparison of the samples.

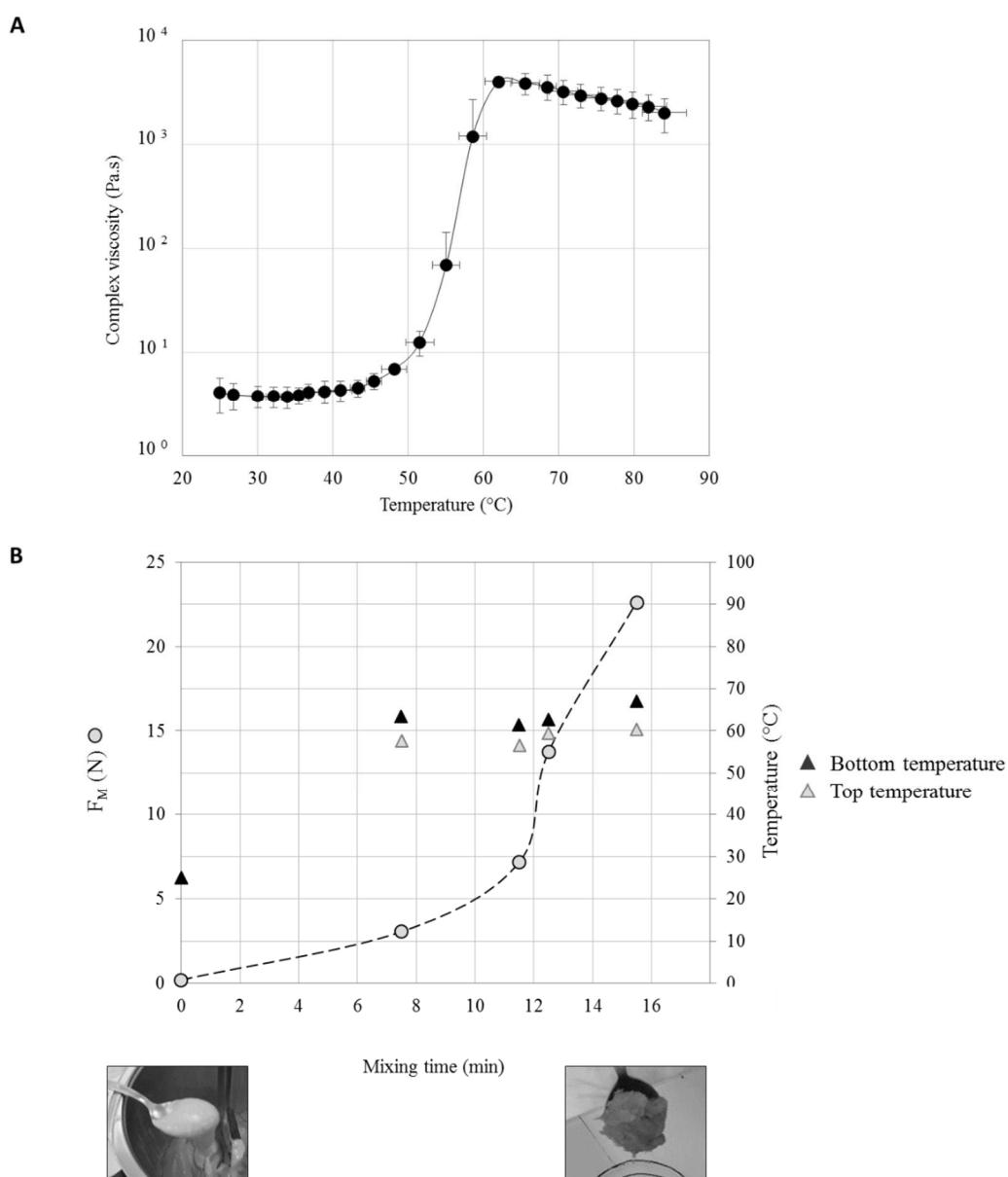
231 **III. Results and discussion**

232 *III.1. Characterization of dough and processed dough made of wheat flour and water*

233 Figure 2.A shows changes in the complex viscosity as a function of temperature for doughs with 65
234 wt% water. The viscosity decreased slightly from 25 to 40 °C, most probably due to a thermal
235 agitation effect (Vanin et al., 2018). Then, between 55 and 65 °C, viscosity increased dramatically to
236 4,000 Pa.s, in good accordance with the literature (Campos et al., 1997; Vanin et al., 2018). DSC
237 measurements identified the temperature required to trigger starch gelatinization (T_{onset}) in this
238 dough to be around 58 °C (± 0.3 °C). **Consequently, the increased viscosity is assumed to be caused**
239 **not only by the absorption of the water and swelling of the starch granules, but also by protein**
240 **aggregation between 50 and 85 °C (Leon et al., 2003).** From 65 °C to 80 °C, viscosity decreased slowly
241 to reach 2,025 Pa.s. The slow decrease in the complex viscosity from 60 to 85°C is hypothesized to
242 reflect the softening of the swollen starch granules (Tsai et al., 1997). The final viscosity was rather
243 close to the viscosity of melted PLA, suggesting that this heated dough has potential for 3D printing.
244 Back extrusion tests were carried out to monitor changes in dough texture during the
245 thermomechanical process used for the production of printable material. Figure 2.B presents F_M and
246 the temperature levels at the bottom and at the surface of the dough as a function of the processing
247 time. A progressive increase in F_M from 0.2 to 7 N occurred from 0 to 11.5 min of thermomechanical
248 treatment. After 11.5 min, F_M increased by a factor 2 in only 1 min to reach 14 N. At the end of the
249 process, F_M was 22 N. Overall, the average temperatures at the surface and at the bottom of the
250 bowl remained relatively stable over time and higher than the theoretical starch T_{onset} measured in
251 the dough, corresponding to the beginning of starch gelatinization. The increased F_M was correlated

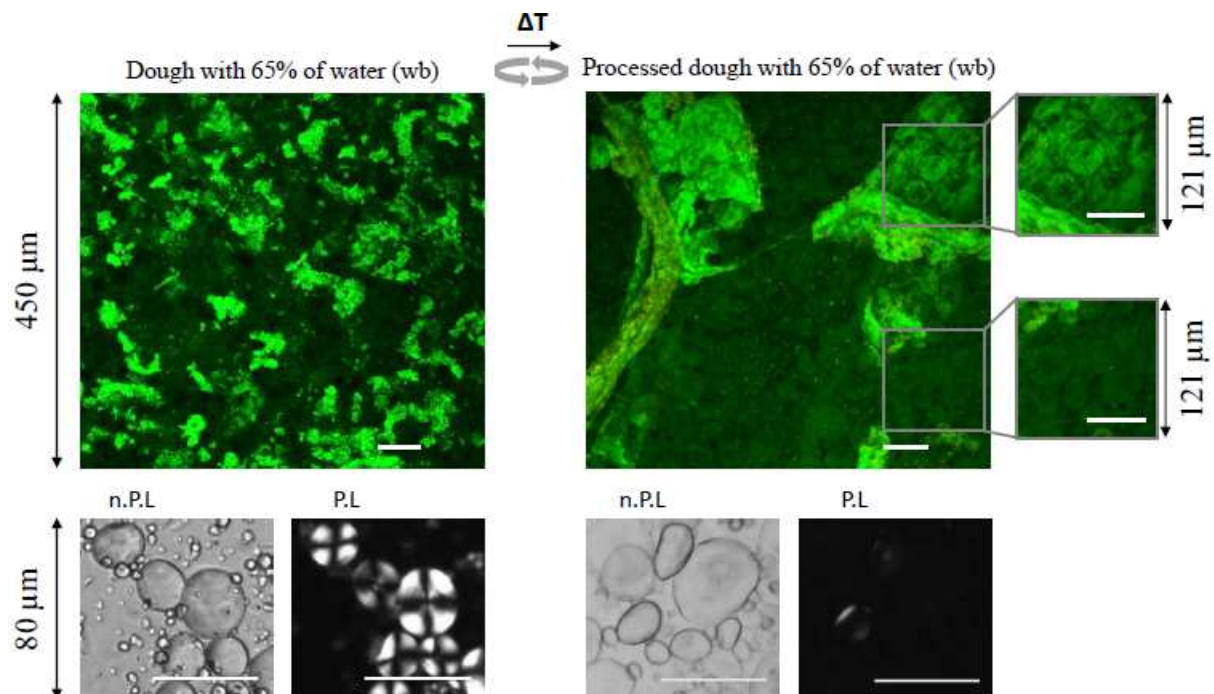
252 with changes in the texture of the dough, which changed from liquid to pasty and sticky as shown in
 253 the pictures taken before and after processing (Figure 2.B).

254 When a suspension of starch and proteins was heated and mixed, shearing led to the formation of
 255 particles composed of swollen gelatinized starch embedded in a continuous gelled phase. The flow
 256 properties of the particle system were evaluated by measuring F_M when the particles were going
 257 through the gap during the back-extrusion test. The particles were invisible to the naked eye but
 258 were expected to be less than 500 μm .



259
 260 *Figure 2: Increase in complex viscosity and normal resistance force (F_M) of dough at 65 wt% of water upon heating. A.*
 261 *Complex viscosity at 1Hz (heating rate: 5 °C/min; 0.2% strain); B. F_M (after cooling) and temperatures at different mixing*
 262 *times.*

263 The microstructure of the dough and processed dough with 65 wt% of water is shown in Figure 3.
 264 The proteins in the dough formed unbound particles > 50 μm in diameter. Mixing conditions and
 265 water content led to the production of unconnected swollen objects made of proteins (Auger et al.,
 266 2008; Masbernat et al., 2021). Starch granules were dispersed in the suspension as shown in diluted
 267 condition with non-polarized light microscopy (n.P.L) (Figure 3). Large and small starch granules with
 268 diameters ranging from 1 to 45 μm were identified, in good agreement with the literature (Raeker et
 269 al., 1998). Under polarized light, starch granules showed the Maltese cross attesting to the semi-
 270 crystalline organization of the macromolecules in the native starch granule (French, 1972).



271
 272 *Figure 3: Observations of the dough with 65% of water after mixing at room temperature (Step 1) and after*
 273 *thermomechanical processing and cooling (Step 3) by CLSM (magnification X10; proteins are stained green) and viewed*
 274 *under polarized light (P.L) and non-polarized light (n.P.L) (magnification X50). All scale bars are 50 μm .*

275 After the thermomechanical treatment, the wheat flour proteins formed large connected objects in
 276 addition to the continuous filler present between the starch granules. With sufficient hydration
 277 during heat treatment, the denaturation of proteins starts with reversible unfolding of glutenins
 278 followed by the formation of disulfide bonds in the glutenins, resulting in the formation of insoluble
 279 protein aggregates containing both gliadins and glutenins (Domenek et al., 2003). When mixing and
 280 heating were combined, the dense aggregates of protein particles connected to each other to form

281 larger strands that were stretched by shearing (Figure 3). The presence of proteins between the
282 starch granules is shown by the green stain observed on the surface of starch. This observation
283 confirms the hypothesis proposed by Mann *et al.* (2014) that denatured gluten aggregates act like
284 weakly interconnected fillers in the starch network when a dough with 40 wt% of water is heated.

285 The photo taken under n.P.L shows swollen granules, whose contours are thin and blurred. The
286 photo taken at the same location under polarized light shows a black background. The loss of
287 crystallinity and the moderate swelling indicate that starch granules gelatinized during the heat
288 treatment, yet the gelatinization appears to be only partial: observation of the microscopic pictures
289 under polarized light shows some granules with crystalline parts near the surface. In the close-up
290 CLSM pictures of the processed dough (Figure 3, on the right), starch granules are embedded in the
291 protein aggregates and are in contact with other granules.

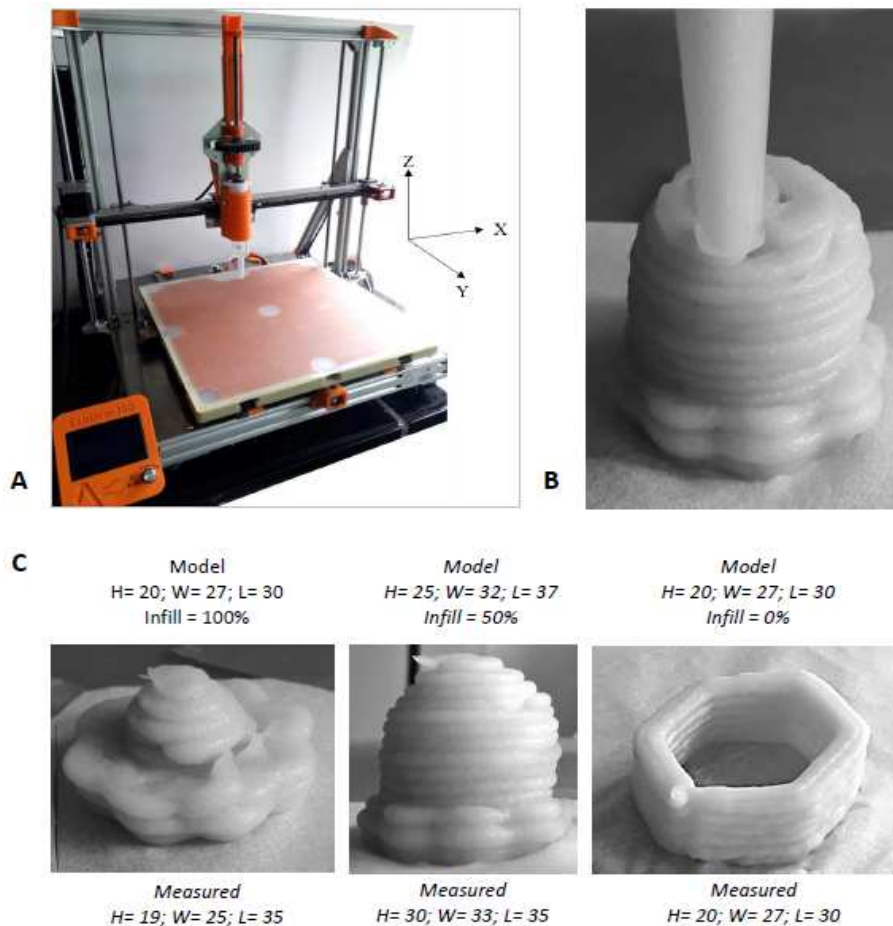
292 These results are evidence that the process modified the state of both starch and proteins by
293 enabling the starch to swell and gluten protein to aggregate. After the process, the swollen starch
294 granules occupied a large proportion of the processed dough and the denatured proteins formed a
295 continuous matrix between the starch granules and long proteins strands, the latter can reach 500
296 μm in length. Similarly to the more dilute heated dough studied by Champenois *et al.* (1998), the
297 denatured protein strands formed areas that prevented contact interaction between granules and
298 delimited cohesive dough particles composed of some swollen starch glued in denatured proteins.
299 These particles occupied all the volume and were sticky. They formed a closely-packed network.

300 **Therefore, the rheological properties of the processed dough are hypothesized** to be determined by
301 the interactions and mechanical properties of these sticky dough particles, that in turn, depend to a
302 great extent on the state of the starch and gluten.

303 The processed dough at 65 wt% of water was printed with a 3D food printer prototype (Figure 4.A).
304 Pictures of the printed objects are shown in Figure 4 (B and C) and their dimensions compared to the

305 corresponding models, showing from 0 to $\pm 17\%$ deviation in length or height, which can be
306 considered satisfactory given the complexity of the printed structure (Yang et al., 2018).

307



308

309 *Figure 4: Pictures of 3D printed objects made of processed dough containing 65 wt% of water after thermomechanical*
310 *processing and cooling. A. 3D printer; B. Printing in progress; C. Examples of printed objects. The height (H), length (L), width*
311 *(W) and infill percentage of the models are given in mm and % above the pictures. The dimensions (mm) measured after*
312 *printing are given under the pictures.*

313 These dimensions remained unchanged five minutes after printing. Thus, with the printing conditions

314 used here, the rheological properties of the processed dough were compatible with 3D food printing.

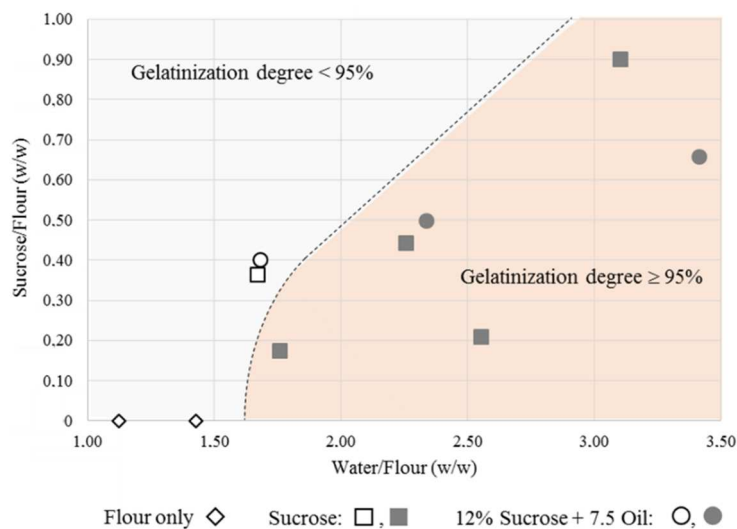
315 Its stickiness could be an advantage for 3D food printing, increasing adhesion between the deposited

316 layers, which is an important parameter in controlling the quality and mechanical properties of

317 printed objects (Chaunier et al., 2018; Vancauwenberghe et al., 2017).

318 *III.2. Impact of adding water, sucrose and oil on the printability of the processed dough*

319 The characteristic gelatinization temperatures (T_{onset} , T_{Max}) measured by DSC for doughs before the
 320 heating step increased with increasing sucrose content, in agreement with the literature (Abboud
 321 and Hosenev, 1984; Perry and Donald, 2002). The degree of starch gelatinization (G) was calculated.
 322 As the proportion of water and sucrose versus starch influence the characteristic gelatinization
 323 temperatures, Figure 5 presents the different points positioned with respect to both the water/flour
 324 and sucrose/flour ratios. Interestingly, two areas with different gelatinization degrees are defined:
 325 one with $G \geq 95\%$, the other one with $G < 95\%$.



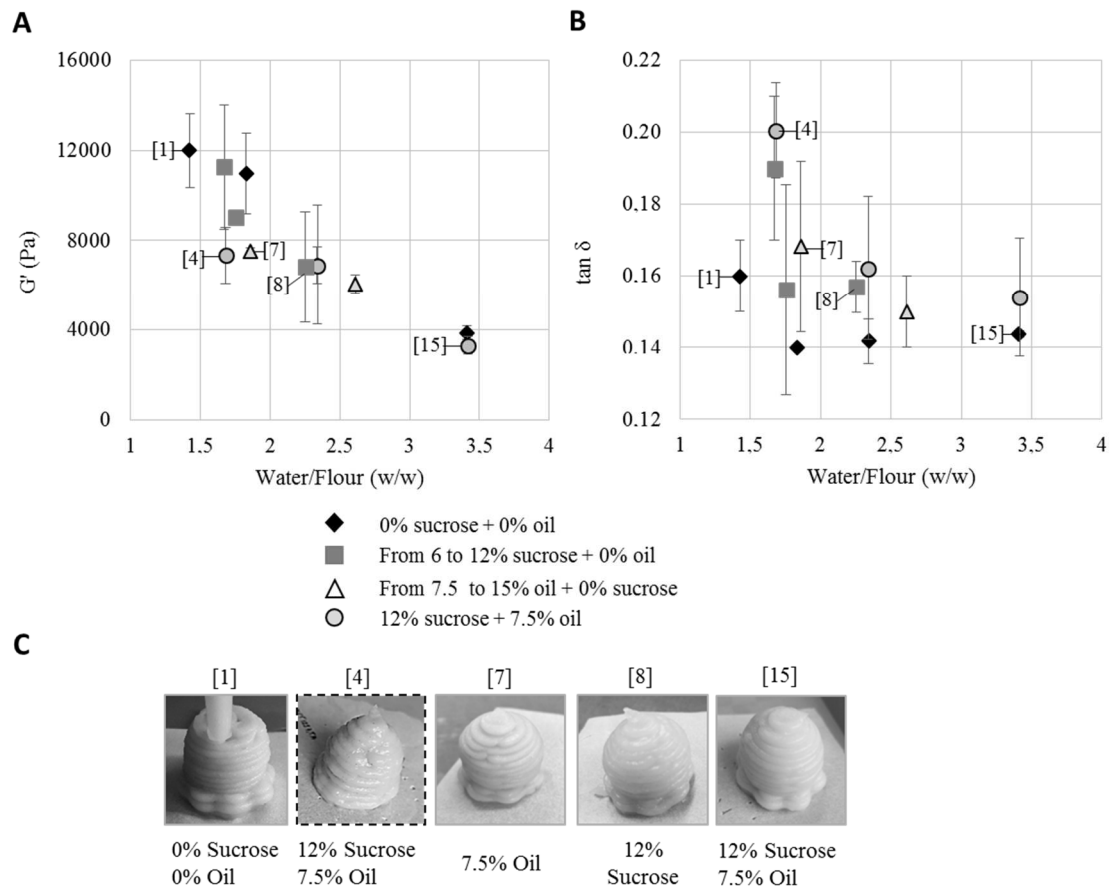
326
 327 *Figure 5: Degree of starch gelatinization in processed doughs with the addition of different quantities of sugar (from 0 to 18*
 328 *wt%), oil (0 or 7.5 wt%) and water (from 55 to 70 wt%). Black symbols, $G \geq 95\%$; empty symbols $G < 95\%$. The dotted line is*
 329 *the estimated water/flour ratio above which starch gelatinization in the processed dough was complete.*

330 Formulation with a water/flour ratio below 1.5 and with no sucrose led to incomplete starch
 331 gelatinization. The result was the same with a water/flour ratio of 1.68 with a sucrose/flour ratio of
 332 0.40, probably due to the increase in T_{onset} and T_{max} . At higher water/flour ratios, whatever the
 333 sucrose/flour ratio, gelatinization was complete due to the larger amount of water available for
 334 starch gelatinization.

335 Non-gelatinized or partially gelatinized starch granules are more rigid than gelatinized ones. The
 336 higher the degree of gelatinization, the softer the starch granules and probably also the dough sticky
 337 particles.

338 Changes in the storage modulus and $\tan\delta$ of the processed doughs are shown as a function of the
339 water/flour ratio (Figure 6.A and 6.B, respectively). G' decreased with an increase in the water/flour
340 ratio, as reported by other authors in starch-concentrated pastes (Hansen et al., 1990). As G' is
341 measured at low deformation, in concentrated particulate systems made of deformable particles, it
342 reflects particle rigidity (Adams et al., 2004; Fridrikh et al., 1996). In the present study, it can be
343 attributed to the greater softness of the starch granules, but also of the protein strands and of the
344 glue between the starch granules due to a lower rate of protein aggregation.

345 It seems that at water/flour ratios above 2.0, adding sucrose and or oil to the dough has no effect.
346 Water content was the most important factor in terms of softening. On the other hand, at
347 water/flour ratios below 2.0, the G' of doughs containing oil was significantly lower than that of
348 doughs containing no oil, which means that oil has a softening effect by itself. This is in good
349 agreement with the results obtained by Agyare and co-authors (2004) in a less hydrated heated
350 dough including shortening. When the dough containing oil was heated, the size distribution of the
351 oil droplets changed and the droplets merged to form a layer of fat around the starch granules
352 (Hesso et al., 2015), which could facilitate slippage between starch granules. The effect of sucrose by
353 itself on G' with this water/flour ratio is less clear. $\tan\delta$ values were all in the range 0.14-0.17 except
354 for dough containing 12 wt% sucrose, which had higher values (0.19 and 0.20). All doughs with $\tan\delta$
355 lower than 1, showed a solid-like behavior. It appears that high sucrose content leads to less
356 structured systems with higher energy dissipation. With the water/flour ratio used here, starch was
357 not completely gelatinized, and the softness of the main starch granules was medium. Thus, the
358 protein strands and glue are probably the structures that are most affected by high sucrose content.



359

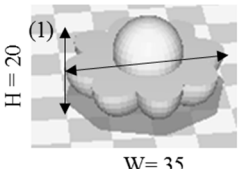
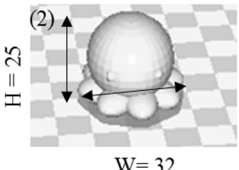
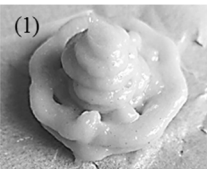
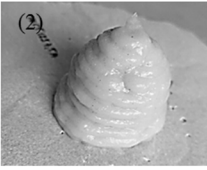
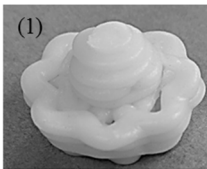
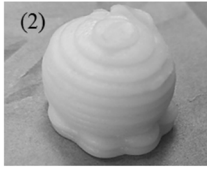
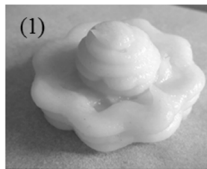
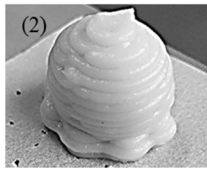
360 Figure 6: Storage modulus (A) and $\tan\delta$ (B) at 1Hz (0.2% of maximum amplitude strain, 20°C) versus
 361 water/flour ratios of processed doughs and pictures of printed objects with different proportions of
 362 flour/water, sucrose and/or oil (C). The picture framed by the black dashed line is an example of
 363 unsatisfactory printing.

364 The printing quality of the objects printed using most of these doughs was satisfactory even if the
 365 range of their G' values was rather wide (3.8-12 kPa) (Figure 6.C). This result is in good agreement
 366 with the literature (Liu et al., 2017; Zhang et al., 2018), in which G' values in the range 4-27 kPa were
 367 positively correlated with shape retention and high resolution of 3D printed objects. However, in this
 368 study, the printing quality of doughs containing 12 wt% of sucrose was average (Figure 6.C, [8]) and
 369 that of doughs containing both 12 w% sucrose and 7.5 w% oil was even worse even though their G'
 370 values were within the G' range of other printable doughs. Interestingly, their $\tan\delta$ was significantly
 371 higher (0.19 and 0.20, respectively).

372

373 The printing quality thus appears to be higher for processed doughs with $\tan\delta$ in the range 0.14-0.17.
 374 To check this hypothesis, values of G' , $\tan\delta$ and shapes of 2 objects are reported and compared in
 375 Table 2 for 3 doughs containing 12 wt% of sucrose and 7.5 wt% of oil and 3 different water
 376 concentrations. Despite the higher G' , the only one with poor printability quality was the dough with
 377 a $\tan\delta$ of 0.20. **Tan δ seems** to be a relevant additional indicator to predict the printing quality of
 378 such doughs.

379 *Table 2: Water/flour ratios and printability of processed doughs including 12 wt% of sucrose and 7.5 wt% of sunflower oil*
 380 *with different total water contents ranging from 55% to 65 wt%.*

	55% of water (wb)	60% of water (wb)	65% of water (wb)
Code number	[4]	[10]	[15]
Storage Modulus (Pa)	7337	6545	3310
$\tan\delta$	0.20	0.16	0.15
Water/Flour (w/w)	1.68	2.34	3.41
<u>Printing:</u> Pictures   Dimensions Height (H) and width (W) after printing (mm)	  (1) : H = 24; W = 26 (2) : H = 30; W = 26	  (1) : H = 23; W = 32 (2) : H = 26; W = 30	  (1) : H = 20; W = 36 (2) : H = 30; W = 32

381
382

383 IV. Conclusion

384 A thermomechanical process was successfully developed to produce wheat flour based printable
 385 material. The combination of mixing and heating led to the formation of closely-packed dough
 386 particles made of swollen starch granules glued in denatured proteins. Logically, the proportions of
 387 water, sucrose and oil affected the mechanical properties of these concentrated particulate systems.

388 The water/flour ratio was found to mainly affect particle rigidity. At the lower water/flour ratio, the
389 oil reduced G' due to slippage, while sucrose increased $\tan\delta$ due by modifying the structure of the
390 protein aggregates. For a wheat flour dough with a G' in the range 3-10 kPa, a $\tan\delta$ in the range 0.15-
391 0.17 appears to be a relevant criterion to predict good printability.

392

393 **V. Acknowledgment**

394 The authors thank Laura Chhour (former student at AgroParisTech, France) for her contribution to
395 the DSC, rheological and printing experiments. This work was supported by Single Inter Ministry Fund
396 (France) and regional co-financing (*Hauts de France* and *Auvergne Rhône Alpes*, France) through a
397 collaborative R&D project certified by Vitagora, Euramaterials and Cimes competitiveness clusters.

398 **VI. References**

- 399 Abboud, A., Hosoney, R.C., 1984. Differential Scanning Calorimetry of Sugar Cookies and Cookie
400 Doughs. *Cereal Chem.* 61, 34-37.
- 401 Adams, S., Frith, W.J., Stokes, J.R., 2004. Influence of particle modulus on the rheological properties
402 of agar microgel suspensions. *J. Rheol. (N. Y. N. Y.)* 48, 1195–1213.
403 <https://doi.org/10.1122/1.1795193>
- 404 Agyare, K., Xiong, Y., Addo, K., Akoh, C., 2004. Dynamic Rheological and Thermal Properties of Soft
405 Wheat Flour Dough Containing Structured Lipid. *J. Food Sci.* 69, 478–487.
- 406 Auger, F., Morel, M.-H., Lefebvre, J., Dewilde, M., Redl, A., 2008. A parametric and microstructural
407 study of the formation of gluten network in mixed flour–water batter. *J. Cereal Sci.* 48, 349–
408 358. <https://doi.org/10.1016/J.JCS.2007.10.006>
- 409 Bagley, E.B., Christianson, D.D., 1982. Swelling capacity of starch and its relationship to suspension
410 viscosity-Effect of cooking time, temperature and concentration. *J. Texture Stud.* 13, 115–126.
- 411 Bakrani Balani, S., Chabert, F., Nassiet, V., Cantarel, A., 2019. Influence of printing parameters on the
412 stability of deposited beads in fused filament fabrication of poly(lactic) acid. *Addit. Manuf.* 25,
413 112–121. <https://doi.org/10.1016/j.addma.2018.10.012>
- 414 Bean, M.M., Yamazaki, W.T., 1978. Wheat starch gelatinization in sugar solutions. I. Sucrose:
415 Microscopy and Viscosity effects. *Cereal Chem.* 55, 936-944.
- 416 Campos, D.T., Steffe, J.F., Ng, P.K.W., 1997. Rheological behavior of undeveloped and developed
417 wheat dough. *Cereal Chem.* 74, 489–494. <https://doi.org/10.1094/CCHEM.1997.74.4.489>
- 418 Champenois, Y., Rao, M.A., Walker, L.P., 1998. Influence of gluten on the viscoelastic properties of
419 starch-gluten pastes and gels. *J. Sci. Food Agric.* 78, 127–133.
420 [https://doi.org/10.1002/\(sici\)1097-0010\(199809\)78:1<127::aid-jsfa99>3.0.co;2-k](https://doi.org/10.1002/(sici)1097-0010(199809)78:1<127::aid-jsfa99>3.0.co;2-k)
- 421 Charun, E.P., Morel, M.-H., 2001. Quelles caractéristiques pour une farine biscuitière ? Influence de

422 la dureté des blés et de la composition biochimique des farines sur leur aptitude biscuitière.
423 Ind. des Céréales n°125, 2–16.

424 Chaunier, L., Guessasma, S., Belhabib, S., Della Valle, G., Lourdin, D., Leroy, E., 2018. Material
425 extrusion of plant biopolymers: Opportunities and challenges for 3D printing . *Addit.*
426 *Manuf.* 21, 220–233. <https://doi.org/10.1016/j.addma.2018.03.016>

427 Coussot, P., Ancey, C., 1999. Rheophysical classification of concentrated suspensions and granular
428 pastes. *Phys Rev E.* 59, 4445–4457.

429 Domenek, S., Morel, M.-H., Redl, A., Guilbert, S., 2003. Rheological investigation of swollen gluten
430 polymer networks: effects of process parameters on cross-link density. *Macromol. Symp.* 200,
431 137–146. <https://doi.org/10.1002/masy.200351014>

432 French, D., 1972. Fine structure of starch and its relationship to the organization of starch granules. *J.*
433 *Japanese Soc. Starch Sci.* 19, 8-25.

434 Fridrikh, S., Raquois, C., Rezaiguia, S., 1996. Rheological behaviour of concentrated suspensions of
435 soft spheres. *J. Chim. Phys. Physico-Chimie Biol.* 93, 941–959.

436 Godoi, F.C., Prakash, S., Bhandari, B.R., 2016. 3d printing technologies applied for food design: Status
437 and prospects. *J. Food Eng.* 179, 44–54. <https://doi.org/10.1016/j.jfoodeng.2016.01.025>

438 Hansen, L.M., Hosney, R.C., Faubion, J.M., 1990. Oscillatory probe rheometry as tool for
439 determining the rheological properties of starch-water systems. *J. Texture Stud.* 21, 213–224.
440 <https://doi.org/10.1111/j.1745-4603.1990.tb00476.x>

441 Hermansson, A.M., Svegmak, K., 1996. Developments in the understanding of starch functionality.
442 *Trends Food Sci. Technol.* 7, 345–353. [https://doi.org/10.1016/S0924-2244\(96\)10036-4](https://doi.org/10.1016/S0924-2244(96)10036-4)

443 Hesso, N., Loisel, C., Chevallier, S., Marti, A., Le-Bail, P., Le-Bail, A., Seetharaman, K., 2015. The role of
444 ingredients on thermal and rheological properties of cake batters and the impact on microcake
445 texture. *LWT - Food Sci. Technol.* 63, 1171–1178. <https://doi.org/10.1016/j.lwt.2015.04.041>

446 Jiang, H., Zheng, L., Zou, Y., Tong, Z., Han, S., Wang, S., 2019. 3D food printing: main components
447 selection by considering rheological properties. *Crit. Rev. Food Sci. Nutr.* 59, 2335-2347.
448 <https://doi.org/10.1080/10408398.2018.1514363>

449 Kim, H.W., Lee, I.J., Park, S.M., Lee, J.H., Nguyen, M.H., Park, H.J., 2019. Effect of hydrocolloid
450 addition on dimensional stability in post-processing of 3D printable cookie dough. *LWT* 101, 69–
451 75. <https://doi.org/10.1016/j.lwt.2018.11.019>

452 Leon, A., Rosell, C.M., De Barber, C.B., 2003. A differential scanning calorimetry study of wheat
453 proteins. *Eur. Food Res. Technol.* 217, 13–16. <https://doi.org/10.1007/s00217-003-0699-y>

454 Leverrier, C., Almeida, G., Espinosa-Muñoz, L., Cuvelier, G., 2016. Influence of Particle Size and
455 Concentration on Rheological Behaviour of Reconstituted Apple Purees. *Food Biophys.* 11, 235–
456 247. <https://doi.org/10.1007/s11483-016-9434-7>

457 Liu, Z., Zhang, M., Bhandari, B., Yang, C., 2017. Impact of rheological properties of mashed potatoes
458 on 3D printing. *J. Food Eng.* 220, 76–82. <https://doi.org/10.1016/j.jfoodeng.2017.04.017>

459 Maache-Rezzoug, Z., Bouvier, J.M., Allaf, K., Patras, C., 1998. Effect of Principal Ingredients on
460 Rheological Behaviour of Biscuit Dough and on Quality of Biscuits. *J. Food Eng.* 35, 23–42.
461 [https://doi.org/10.1016/S0260-8774\(98\)00017-X](https://doi.org/10.1016/S0260-8774(98)00017-X)

462 Mann, J., Schiedt, B., Baumann, A., Conde-Petit, B., Vilgis, T.A., 2014. Effect of heat treatment on
463 wheat dough rheology and wheat protein solubility. *Food Sci. Technol. Int.* 20, 341–351.

464 <https://doi.org/10.1177/1082013213488381>

465 Masbernat, L., Berland, S., Almeida, G., Michon, C., 2021. Stabilizing highly hydrated wheat flour
466 doughs by adding water in two steps. *J. Cereal Sci.* 98, 103179.
467 <https://doi.org/10.1016/j.jcs.2021.103179>

468 Mongondry, P., Tassin, J.F., Nicolai, T., 2005. Revised state diagram of Laponite dispersions. *J. Colloid*
469 *Interface Sci.* 283, 397–405. <https://doi.org/10.1016/j.jcis.2004.09.043>

470 Moussier, M., Huc-Mathis, D., Michon, C., Bosc, V., 2019. Rational design of a versatile lab-scale
471 stirred milk gel using a reverse engineering logic based on microstructure and textural
472 properties. *J. Food Eng.* 249, 1–8. <https://doi.org/10.1016/j.jfoodeng.2018.12.018>

473 Perry, P., Donald, A., 2002. The effect of sugars on the gelatinisation of starch. *Carbohydr. Polym.*
474 49, 155–165. [https://doi.org/10.1016/S0144-8617\(01\)00324-1](https://doi.org/10.1016/S0144-8617(01)00324-1)

475 Quemada, D., 2006. Modélisation rhéologique structurelle : dispersions concentrées et fluides
476 complexes. Lavoisier.

477 Quemada, D., 1977. Rheology of concentrated disperse systems and minimum energy dissipation
478 principle - I. Viscosity-concentration relationship. *Rheol. Acta* 16, 82–94.
479 <https://doi.org/10.1007/BF01516932>

480 Raeker, M.Ö., Gaines, C.S., Finney, P.L., Donelson, T., 1998. Granule size distribution and chemical
481 composition of starches from 12 soft wheat cultivars. *Cereal Chem.* 75, 721–728.
482 <https://doi.org/10.1094/CCHEM.1998.75.5.721>

483 Rao, M.A., 2007. *Rheology of Fluid and Semisolid Foods Principles and Applications*, Gustavo V. ed,
484 Food Engineering Series. https://doi.org/10.1007/978-1-4614-9230-6_6

485 Rapaille, A., Vanhemelrijck, J., 1997. Modified starches, in: *Thickening and Gelling Agents for Food*.
486 Springer US, Boston, MA, pp. 199–229. https://doi.org/10.1007/978-1-4615-2197-6_10

487 Severini, C., Azzollini, D., Albenzio, M., Derossi, A., 2018. On printability, quality and nutritional
488 properties of 3D printed cereal based snacks enriched with edible insects. *Food Res. Int.* 106,
489 666–676. <https://doi.org/10.1016/j.foodres.2018.01.034>

490 Severini, C., Derossi, A., Azzollini, D., 2016. Variables affecting the printability of foods: Preliminary
491 tests on cereal-based products. *Innov. Food Sci. Emerg. Technol.* 38, 281–291.
492 <https://doi.org/10.1016/J.IFSET.2016.10.001>

493 Tsai, M.L., Li, C.F., Lii, C.Y., 1997. Effects of granular structures on the pasting behaviors of starches.
494 *Cereal Chem.* 74, 750–757. <https://doi.org/10.1094/CCHEM.1997.74.6.750>

495 Turner, B.N., Strong, R., Gold, S.A., 2014. A review of melt extrusion additive manufacturing
496 processes: I. Process design and modeling. *Rapid Prototyp. J.* 20, 192–204.
497 <https://doi.org/10.1108/RPJ-01-2013-0012>

498 Vancauwenberghe, V., Katalagarianakis, L., Wang, Z., Meerts, M., Hertog, M., Verboven, P.,
499 Moldenaers, P., Hendrickx, M.E., Lammertyn, J., Nicolaï, B., 2017. Pectin based food-ink
500 formulations for 3-D printing of customizable porous food simulants. *Innov. Food Sci. Emerg.*
501 *Technol.* 42, 138–150. <https://doi.org/10.1016/j.ifset.2017.06.011>

502 Vanin, F.M., Lucas, T., Trystram, G., Michon, C., 2018. Biaxial extensional viscosity in wheat flour
503 dough during baking. *J. Food Eng.* 236, 29–35. <https://doi.org/10.1016/j.jfoodeng.2018.05.007>

504 Wang, L., Zhang, M., Bhandari, B., Yang, C., 2018. Investigation on fish surimi gel as promising food
505 material for 3D printing. *J. Food Eng.* 220, 101–108.

- 506 <https://doi.org/10.1016/j.jfoodeng.2017.02.029>
- 507 Yang, F., Zhang, M., Prakash, S., Liu, Y., 2018. Physical properties of 3D printed baking dough as
508 affected by different compositions. *Innov. Food Sci. Emerg. Technol.* 49, 202–210.
509 <https://doi.org/10.1016/j.ifset.2018.01.001>
- 510 Zhang, L., Lou, Y., Schutyser, M.A.I., 2018. 3D printing of cereal-based food structures containing
511 probiotics. *Food Struct.* 18, 14–22. <https://doi.org/10.1016/j.foostr.2018.10.002>
- 512